

GEOS 5473 : Final Project

An exploration of the potential impacts of future extreme heat events using nonstationary extreme value analysis and temperature-duration-frequency curves

April Walker

University of Arkansas, Fayetteville

Background & Summary

Extreme temperature events and extended periods of extreme heat can have catastrophic impacts on society be it through agriculture, infrastructure and energy production, ecological balance, or direct human health.^{7,8,10,13,14} While anthropogenic climate change is summarized as an increase in the global mean temperature, the spatial risks associated with a changing climate differ drastically. In order to adequately prepare for climate variability, we must accurately predict the potential intensity, duration, and frequency of future climate extremes and determine how specific extremes could impact our society.

Recent research has lead to the development of various heatwave indices. While some directly focus on how heatwaves could impact human health, others attempt to spatially and temporally generalize heatwaves and "warm-spells" (thus including scenarios such as warm winters, or extremes in cooler climates).¹⁴ While these indices do include a vague concept of duration through the inclusion of a three-day-averaged mean daily temperature, they lose information regarding the potential impacts of various durations of temperature extremes. That is, while a three-day-averaged mean is relevant to studying a heat events impact on human health,^{7,13,14} it may be less informative in another context. Additionally, while they may be useful in quantifying past heat extremes, they are less useful at determining the spatial risks associated with climate extremes and determining if these level and frequency of extremes are changing over time.

While it is difficult to assess the direct impact future heat waves could have on the public health, understanding the potential risks allows adequate readiness if they do occur. As is, heat waves have the potential to impact various sectors, therefore, a more specific understanding of future climate projections can allow individual industries to prepare.^{7,13} During extreme heat events, disruption in electricity are more common.^{7,10} While this is more likely due to direct damage to infrastructure, heat waves may also impact the efficiency of water used to cool power plants. As the European heatwave of 2003 affected Europe, France shut down six power plants due to river temperatures reaching record highs. Increased water temperatures, along with varying availability of water resources can be devastating to nuclear power generation.¹⁰ Without adequate availability of electricity, populations are left vulnerable to the impacts of heat waves. Additionally, heat extremes and temperature anomalies and stress crop yields, potentially leading to additional burdens on society.^{7,8}

With the improvement of technology, cities have become less sensitive to extreme heat events even with the events becoming more common.⁷ Of course, this is highly related to factors such as a city's response plan, the accessibility of cooling, and the impact of the urban heat island effect. In addition to the expected impact heat waves have on human health, it has been found that heat waves also contribute negatively to the air quality, which in time contributes to the morbidity from other diseases.^{7,10}

The overarching goal of this project is to learn more about the potential hurdles I'll need to overcome in order to utilize non-stationary extreme value analysis in both particular scenarios to answer complex problems related to temperature extremes, as well as overarching cases to determine the risk of temperature extremes. In order to meet this goal, my first task involves generalizing the state of extremely high temperatures by determining trends and fitting the annual maximum dataset to the General Extreme Value distribution in order to determine return levels for various return periods. The second portion of my study involves developing Temperature-Duration-Frequency (TDF) curves in locations which have significant trends. Specifically, I chose Sacramento, California and Houston, Texas as these locations both have naturally warm and annual maximum temperatures which are significantly increasing.⁷ However, the potential catastrophes associated with these extremes differs significantly. The especially recent Camp Fire outside Paradise, California is a brutal reminder us of the potential risks of drought combined with extreme heat events. In contrast, Houston's climate tends towards humid extreme temperatures, which decreases the bodies ability to cool itself and increases the chance of a heat event impacting human health. Additionally, both locations containing dense metropolitan populations allowing for study on the urban heat island effect. Lastly, these locations contain many additional stations in close proximity which could be added in a more comprehensive study.

Methods

In order to generalize temperature trends in the United States, monthly minimum and maximum temperature data from the National Climate Data Center (NCDC) Climate Divisions was accessed. The following method was applied to all divisions in the contiguous United States. In order to consider an appropriate chosen time frame was, trends were determined for varying durations with 10-year increments beginning at 10 years and ending at 100 years. The standard for defining climate is generally weather averages over a period of at least 30 years. Therefore, In order to develop significant results regarding climate, I considered this my baseline. While this duration is sufficient for general studies regarding climate trends, since I was only extracting one data point per year, I instead chose durations of 40 and 60 years. While a full study of each 10-year increment is not included, it should be noted that trends, especially those for the maximum temperature, were relatively sensitive to this chosen duration. Since the only factor considered correlated with temperature in this study was time, the impact of other climate forcings¹¹ is left uncertain.

All models and methods below were developed using the R package *extRemes* which was funded by the National Science Foundation (NSF) through the NCAR Weather and Climate Impact Assessment Science Initiative with additional support from the NCAR Geophysical Statistics Project (GSP).

In order to apply the General Extreme Value (GEV) distribution to my data, in each climate division the yearly maximum temperature (either for the monthly minimum or monthly maximum dataset) was determined. For each division the Mann-Kendall trend test was applied to the developed yearly maximum time series, with non-stationarity being assumed at a 95% confidence level.

The GEV distribution includes the family of Gumbel, Frchet, and Weibull distributions with their distinction being dependent on the parameters chosen. The following gives the cumulative distribution of the GEV :

$$\Psi(x) = \exp\left\{ -\left(1 + \xi\left(\frac{x - \mu}{\sigma}\right)^{-1/\xi}\right)\right\}, \quad 1 + \xi\left(\frac{x - \mu}{\sigma}\right) > 0$$

In which the location parameter (μ) impacts the central position of the distribution, the scale parameter (σ) impacts the spread or magnitude of the deviations around the center of the distributions, and the shape parameter (ξ) influences the behavior of the tail of the distribution. That is, it impacts where and if the ends of the distribution are highly bounded. To put it in terms of climate extremes, a time series which predicts a tail that is not highly bounded can expect more extremes. If it is approximated that $\xi \rightarrow 0$ then the distribution

becomes the Gumbel distribution shown below :

$$\Psi(x) = \exp\left\{-\exp\left(-\left(\frac{x-\mu}{\sigma}\right)\right)\right\}, \quad -\infty < x < \infty$$

Otherwise, $\xi > 0$ and $\xi < 0$ tend towards the Frèchet and Weibull distributions respectively. To define how the ξ impacts the tail, it should be noted that the Frèchet distribution will result in a heavy upper tail whilst the Weibull distribution will have a bounded upper tail.^{1,3,6}

In order to fit the data to these distributions, it should be considered whether to include the Gumbel distribution. One standard way of fitting the data would include first using the likelihood ratio test, which favors simpler models.⁶ By using this method, the process will only favor the GEV over the Gumbel if it passes the likelihood ratio test with a confidence level of 95%. On the contrary, it could be argued that the probability of ξ being equivalent to an exact value is zero (i.e. $\xi = 0$) and thus the hypothesis should be whether $\xi = 0$ or $\xi \neq 0$.^{5,6} For the first dataset (the contiguous United States), I applied the likelihood test to the Gumbel distribution before applying any other conditions or covariates to my parameters. In the second study, I instead set the distribution to be GEV. This, of course, does not mean that the shape parameter will not take on a low value, but rather that it is not explicitly set to zero.

If the trend fitting process and Mann Kendall test determined a location to have non-stationary annual maxima, various models were applied to the data and the best-fit was determined. The below table shows the various correlations the variables could take on :

$$\begin{aligned}\tau(i) &= \frac{Year(i) - Year(1)}{n} \\ \mu(i) &= \mu_0 + \tau(i)\mu_1 + \tau(i)^2\mu_2 \\ \sigma(i) &= \sigma_0 + \tau(i)\sigma_1 + \tau(i)^2\sigma_2 \\ \xi(i) &= \xi_0\end{aligned}$$

That is, τ takes on some value between 0 and 1 representing the percentage of time passed since the beginning of the dataset to the end. Both μ and σ are allowed to vary with time, however ξ is fixed. This decision is based partially on previous studies decisions, however testing also showed interesting but unusual results when ξ was allowed to vary. Additionally, σ arguably also developed unusual results when allowed to vary quadratically in time, and was at one point taken out. However, without a definitive reason to disclude σ , I decided to allow it to vary quadratically.^{2,12} Additional study may be advised in this area.

In order to decide the appropriate fit for the models, the Akaike information criterion (AIC) was used. This value allows you to test the quality of a statistical model in comparison to another model, with preference given to the simpler models. This negates some of the probability of overfitting caused by choosing a model with unnecessary parameters. If we define a $\psi = \{\mu, \sigma, \xi\}$, we can estimate the number of parameters by computing the Hessian sensitivity matrix and the variability matrix of ψ . Sometimes, this computation fails, and instead the negative log-likelihood is used. In both cases, the chosen model should have their fit criterion the closest to zero. For the study involving the contiguous United States, if a quadratic model was chosen, it was rechecked against the best-fitting linear model using the likelihood ratio test using a standard of 95% confidence. The only models which failed the test tended to lie within 90% confidence level, and also tended to not have a computational AIC. For the smaller study building TDF curves, this process was deemed unnecessary as all models developed AIC values. These models were forced back to the best-fitting linear model. In addition to this, models were visually checked using quantile-quantile (Q-Q) plots.^{2,4,12}

Once the data was fitted to models, return level plots were developed. In this study, return level refer to the extreme high temperature predicted by the model in a given period. The given period for a given return level is called the return period. For each climate division return level plots were developed for 2, 20, and 100 year durations in order to give an appropriate view of the expected extremes (and changes of extremes) for a short, intermediate, and long period of time.^{1,6}

For the portion of this study involving the development of TDF curves, a very similar process to the above

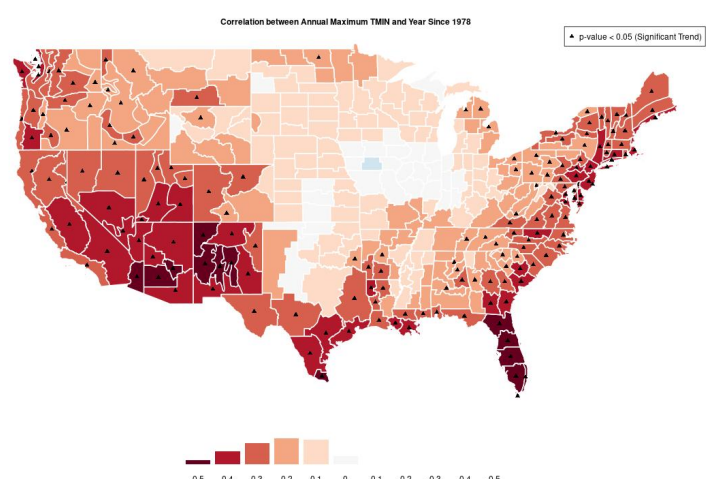
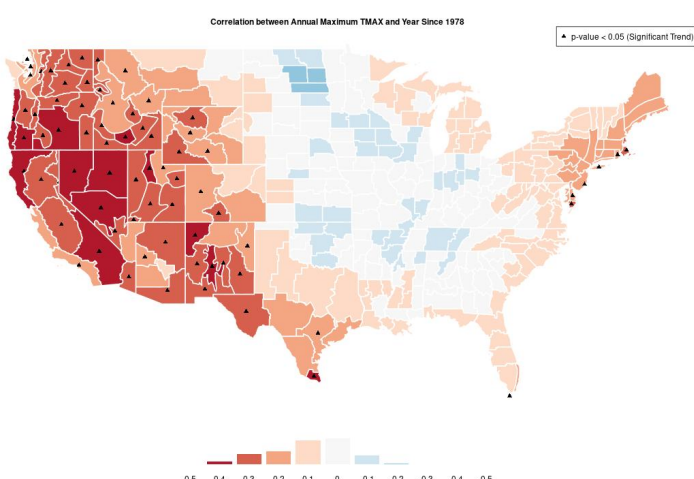
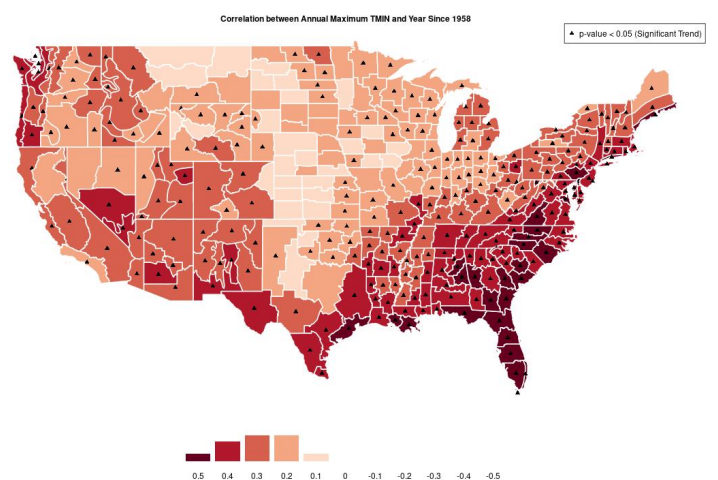
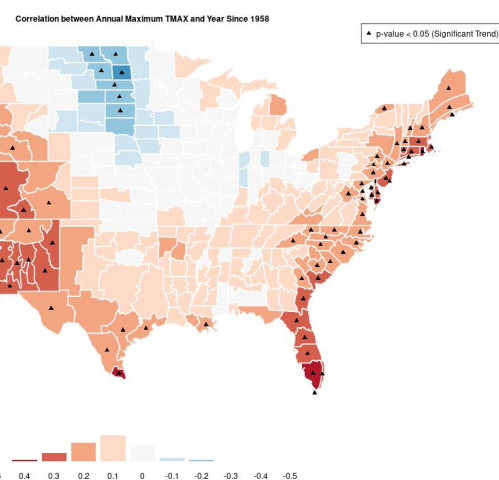
was used, with a few variations. Rather than only compute the maximum for a one duration event, the maximum was computed for a rolling average of durations $D = \{1, 2, \dots, 7, 10\}$ days, that is a total of 8 durations. The ones that will be specifically shown below are 1, 3, and 7 days in order to give a picture of the variation between durations. For this study, confidence intervals of 95% were also computed. This process was specific inspired by two previous studies, one by Ouarda, T. B., Charron, C. (2018), the other by Cheng, L., Aghakouchak, A. (2014).

For the TDF, data was taken since 1958 from the NCDC's Global Historical Climate Network Daily Database. Since a single location did not have reasonably complete data (over 99%), two close by locations (station code USW00012906 and USW00012918) and combined in 1970. A further analysis was not done to see how this could have impacted the results. Due to their proximity this was considered negligible, but in future studies should be a factor of consideration when performing error analysis. For Sacramento, one station (USW00023271) had reasonably complete data (over 99%) to analyze since 1958.

In analyzing this data, rather than utilize a dataset spanning the entire year, solely the summer months were studied (June, July, and August). To compute the rolling averages, each average was centered or approximately centered on the specified day. Therefore, in computing the longer duration averages, the total time-span included had a minimum start date of May 28th and a maximum end date of September 5th.

Results

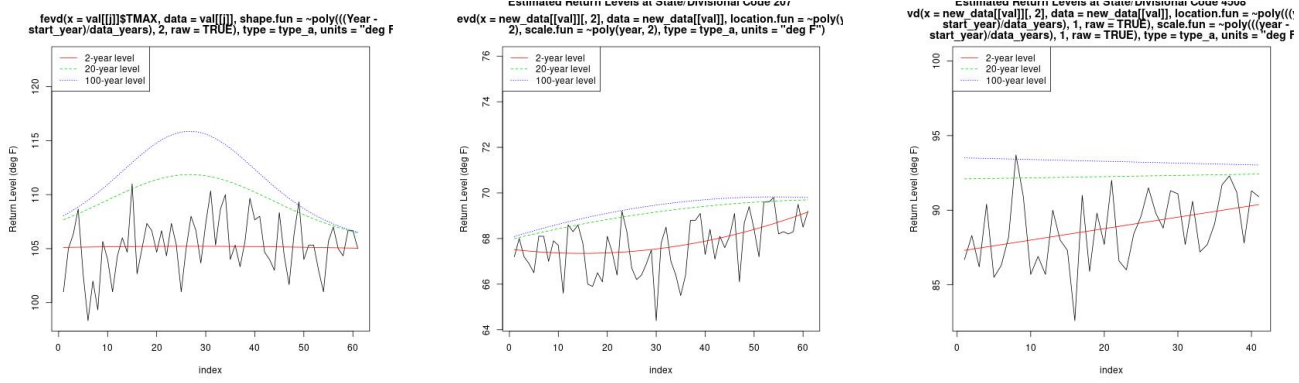
The following charts were developed showing the correlation between temperature and time for the data beginning in 1958 and 1978, with the charts since 1958 preceding the later. For each duration, the left charts show the annual maximum monthly maximum and the right charts show the annual maximum monthly minimum for the climate divisions. Note that the color is determined by the Mann Kendall's correlation coefficient, not the significance value. Therefore, the 1958 chart's color does not necessarily determine significance at the same level as the 1978 chart.



While seemingly not as important as the monthly maximum, the monthly minimum could be an important feature to consider when studying heatwaves, as a feature of many of the most catastrophic heatwaves was the high night time temperatures exacerbating the impacts of the extreme daily temperatures. Further study could also be done to determine the change of trends for each season, a shed light on issues such as the changes springtime melt and snowfall/precipitation ratios.

In both durations, considerably significant trends were found, especially for the monthly minimum dataset. These locations with significant trends are indicated with a triangle over their respective region. Once the models are fitted it should be noted that only these locations will have non-stationary models.

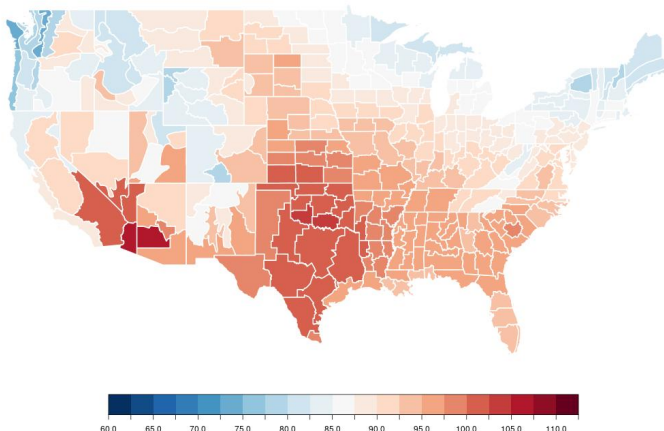
During the fitting process it was determined that quadratic models especially had the tendency of over-fitting, even with the various fitting criterion in place. Thus, the following page will show maps which allowed both quadratic and linear models, and maps which excluded the quadratic models. To show the types of over-fitting that occur, below I have 3 examples of raw return level plots developed through this process. While these models may fit the data, they are not robust enough to make predictions about future events.



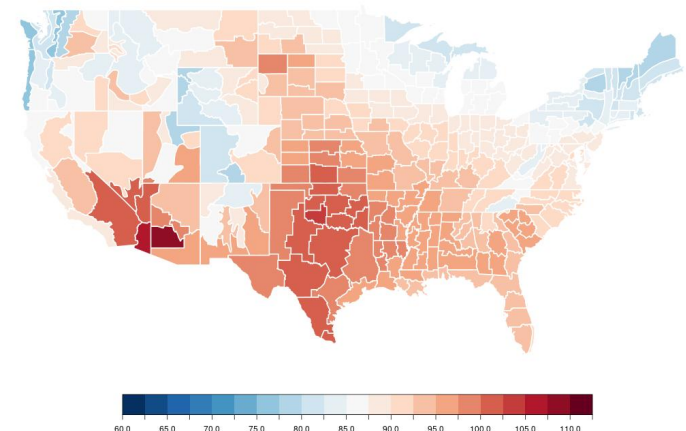
I had noted before that allowing the shape (ξ) parameter to vary would lead to unusual fits. The left most plot above gives such an example. On the other hand, the right most plot gives an example of how even the linear plots may tend towards unusual conclusions with low amounts of data. Over time, we see the red 2-year return level prediction overtakes the 20-year and even 100-year return level events. While the overall trend of annual extremes may be increasing with time, if a few (even one) more extreme event occurred further back in the dataset, it could skew the model to assume these longer return period events are decreasing with time. A similar blunder can occur using quadratic fits, as shown in the middle plot.

Starting at the top, the following page contains maps containing the predicted return level in 1978 and in 1958 for a 20-year event with the former on the left and the latter on the right. Below that are shown the 20-year changes in return level for 1978 and 1958, with linear plots on the left and quadratic models included on the right. Note that the maps including quadratic models did not exclude linear models, only that quadratic models were not specifically excluded like within the linear model chats. The grey areas indicate the the model was stationary, and thus the change is zero. Since the 1978 maps did not differ as significantly depending on the chosen model, only the linear models are shown. The average change shown in the 2018 change maps includes the location which are considered stationary, meaning the median value is generally 0. The following page is identical to this page, however it shows the changes for the monthly minimum dataset while the prior shows the changes for the monthly maximum dataset. It should be noted that the monthly minimum and the monthly maximum are on different temperature scales in the first graph indicating return levels.

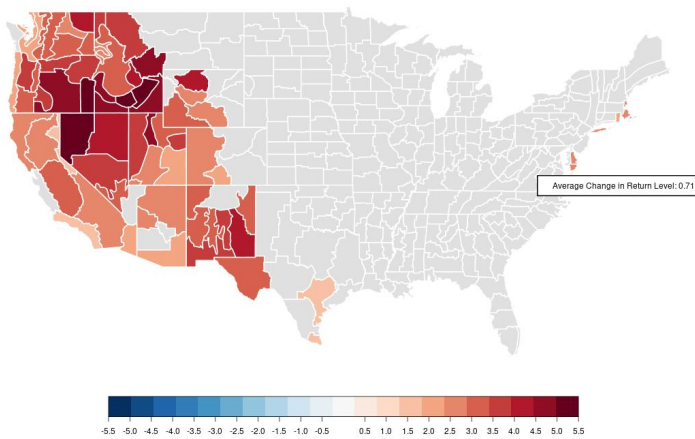
Expected Maximum Return Levels for 20 Years for TMAX in 1978 Using Linear Models



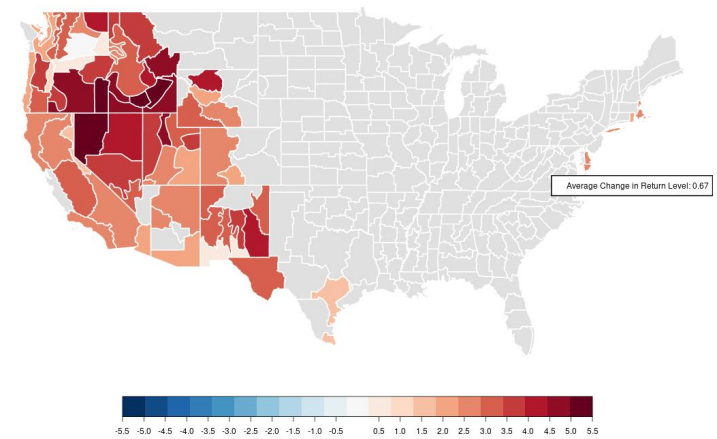
Expected Maximum Return Levels for 20 Years for TMAX in 1958 Using Linear Models



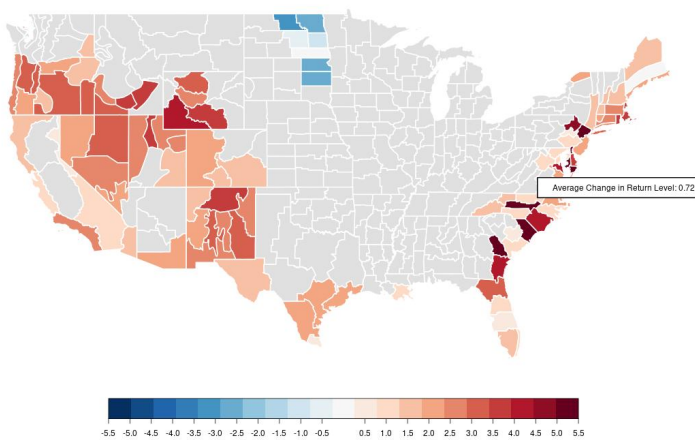
The Change in Expected Maximum TMAX Return Levels for 20 Years Between 1978 and 2018 Using Linear Models



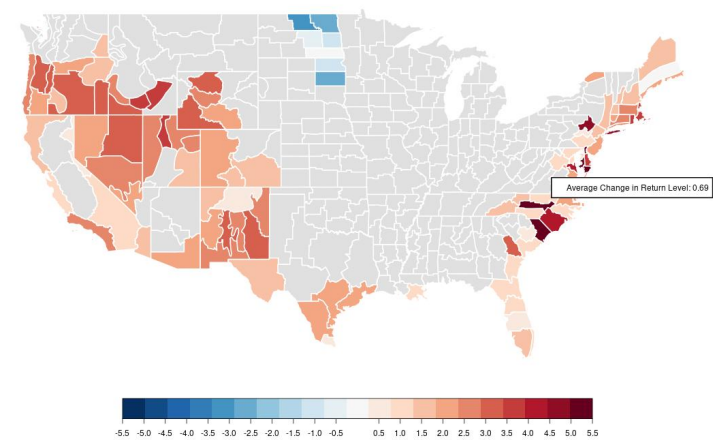
The Change in Expected Maximum TMAX Return Levels for 20 Years Between 1978 and 2018 Using Quadratic Models



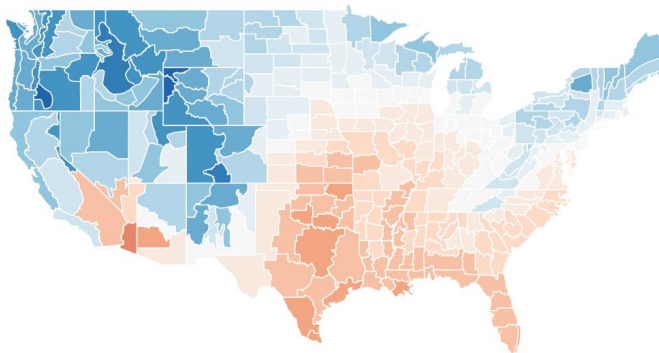
The Change in Expected Maximum TMAX Return Levels for 20 Years Between 1958 and 2018 Using Linear Models



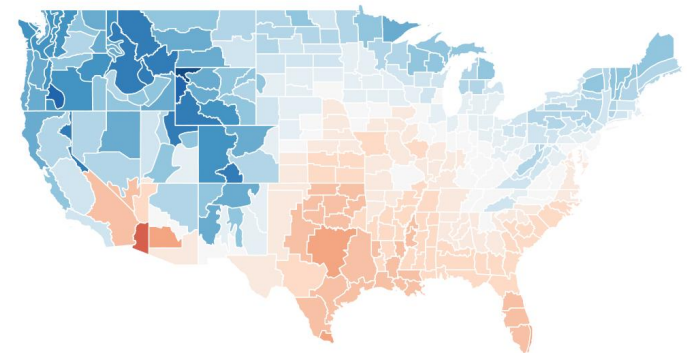
The Change in Expected Maximum TMAX Return Levels for 20 Years Between 1958 and 2018 Using Quadratic Models



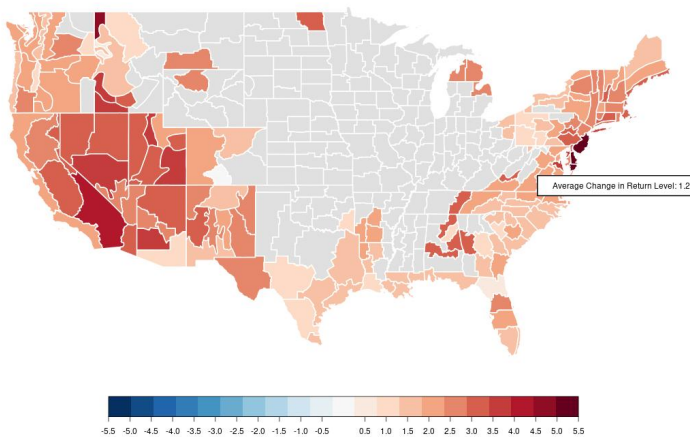
Expected Maximum Return Levels for 20 Years for TMIN in 1978 Using Linear Models



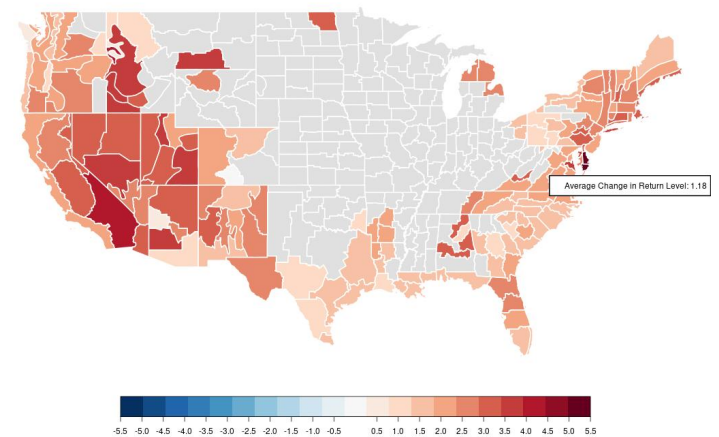
Expected Maximum Return Levels for 20 Years for TMIN in 1958 Using Linear Models



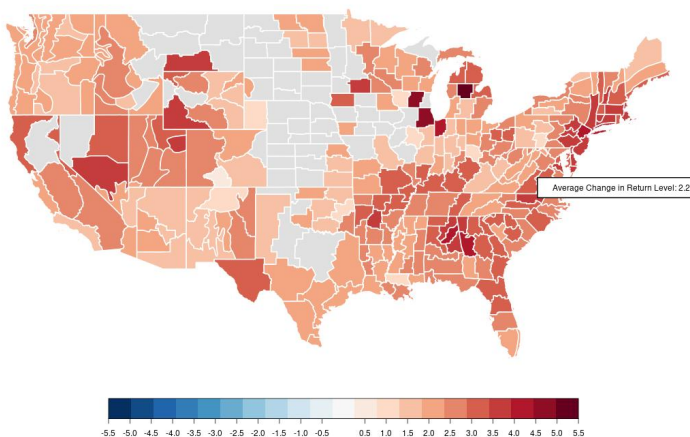
The Change in Expected Maximum TMIN Return Levels for 20 Years Between 1978 and 2018 Using Linear Models



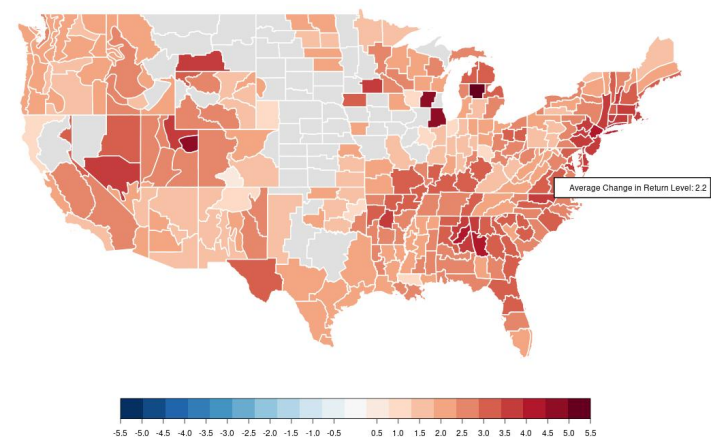
The Change in Expected Maximum TMIN Return Levels for 20 Years Between 1978 and 2018 Using Quadratic Models



The Change in Expected Maximum TMIN Return Levels for 20 Years Between 1958 and 2018 Using Linear Models



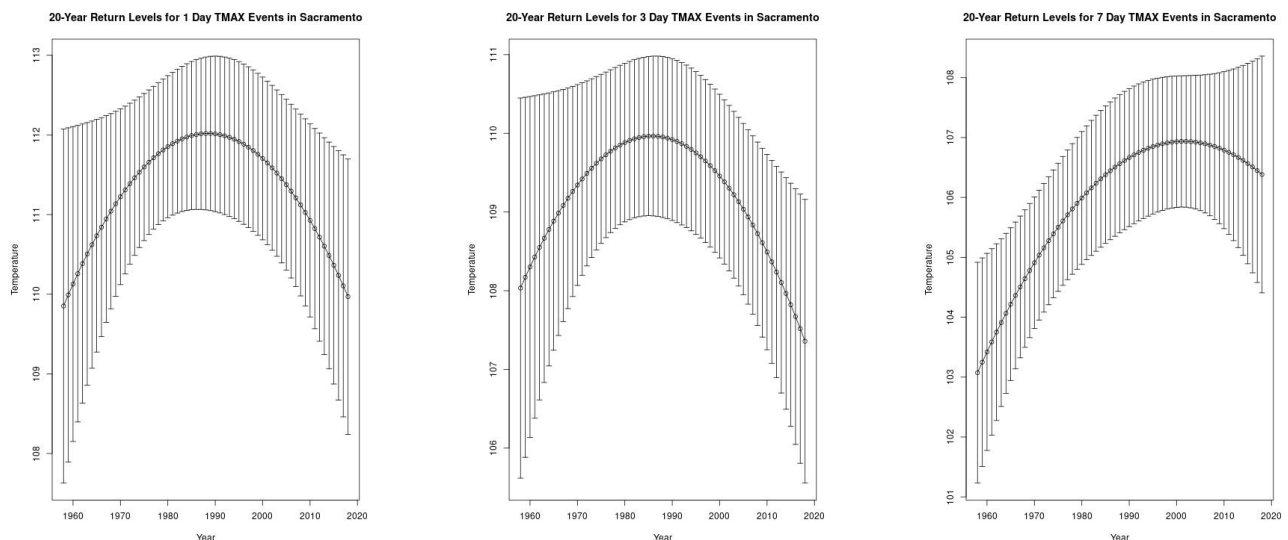
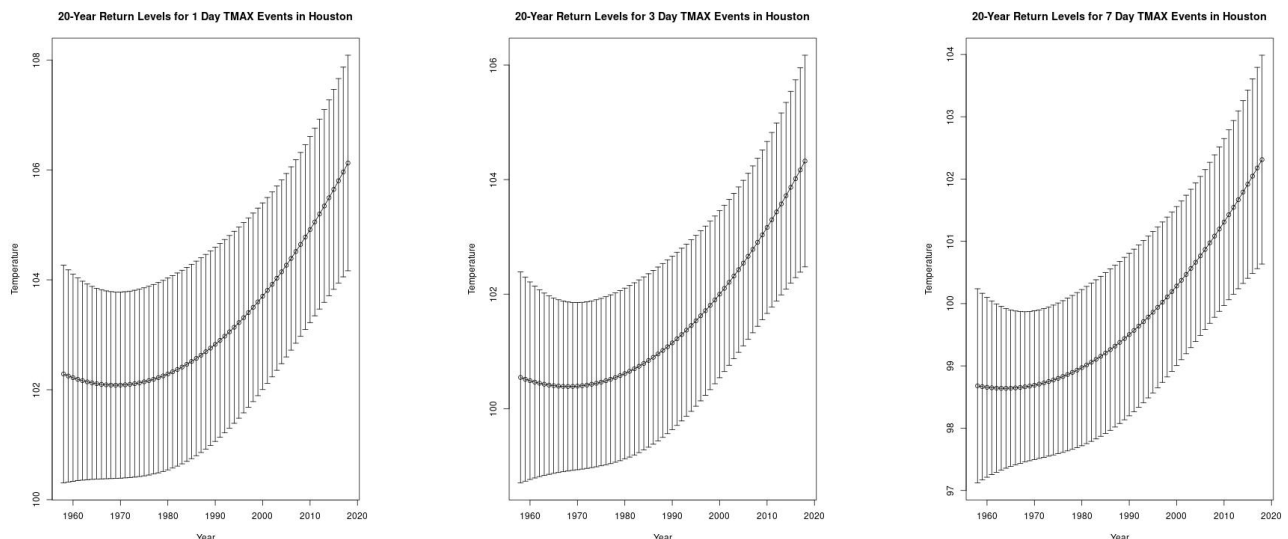
The Change in Expected Maximum TMIN Return Levels for 20 Years Between 1958 and 2018 Using Quadratic Models

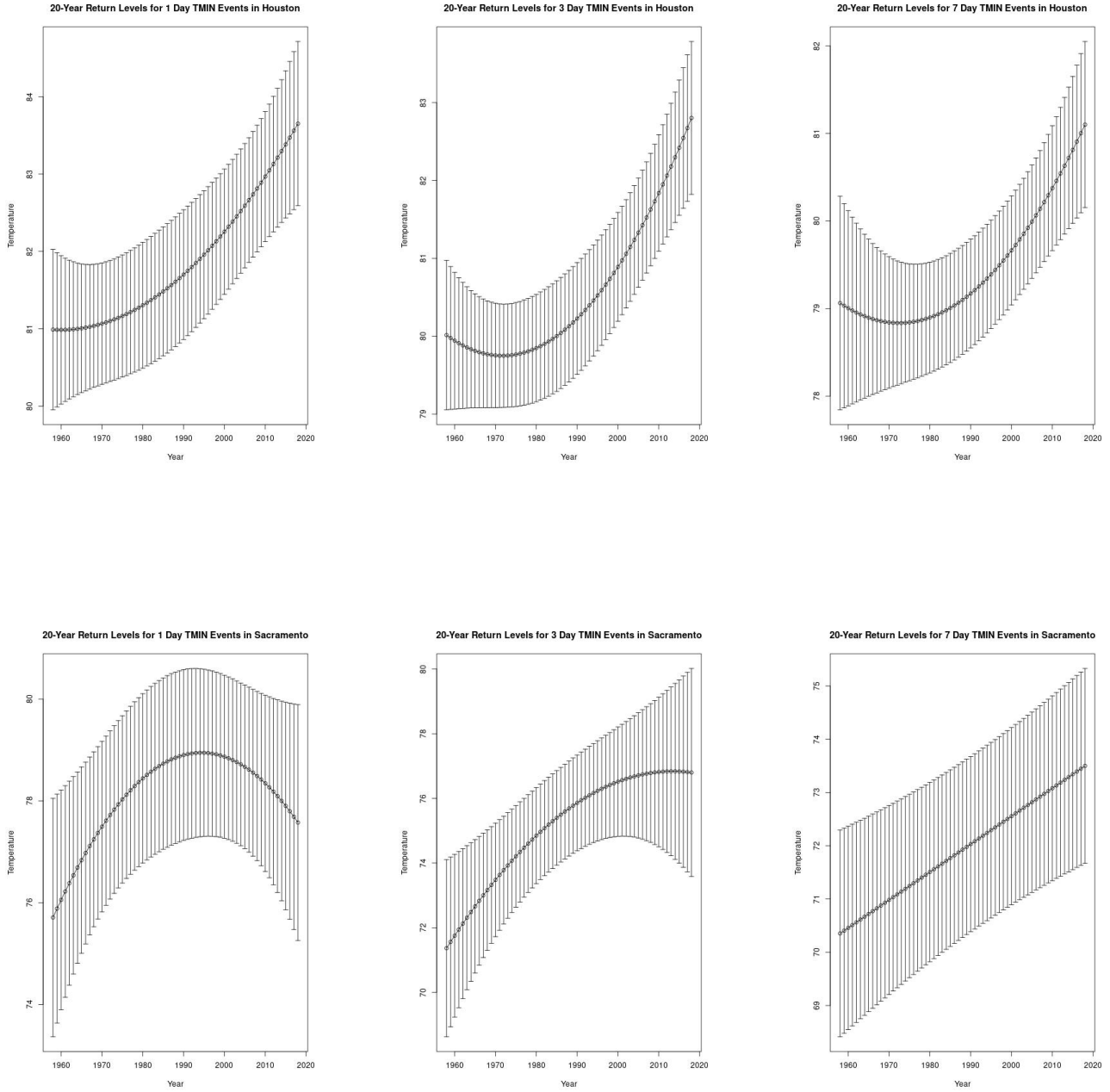


Additional graphs will be available in the appendix. Specifically, linear models indicating the determined return levels for 2-year and 100-year return periods. While not included, it should be noted that the inclusion of the quadratic models in determining the 2-year return levels had little impact on the results, while the quadratic models had similar and sometimes slightly more extreme impacts on the 100-year return level plots. However, given the method used and the short duration of the dataset studied, a 100-year prediction seems very presumptuous.

While not necessarily original, the findings related to the changes in monthly minimum temperatures have especially sparked my interest. Relating this issue to heat waves, warm night time temperatures in conjunction with extreme daytime temperatures pose a massive risk to public health. This is an especially prominent issue in locations prone to the urban heat island impact. A study such as this could make use of the methods added in the additional portion of my study involving a TDF curve on specific metropolitan locations.

For the next portion of my study, the following TDF curves were developed. While curves were developed for time-spans of 2, 20 and 100 years, the only ones shown below are the 20 year curves. The return level curves for the additional return periods are available in the appendix. The first plots shown are the maximum daily temperature curves for durations of 1, 3, and 7 days, with the curves from Houston being shown in the first row and Sacramento curves shown in the second. The following plots are the minimum daily temperature curves, however note this study is still focusing on annual maximums for that dataset. The minimum daily temperature curves follow the same pattern as the above maximum daily temperature curves.





With the exception of Sacramento's 1-day and 3-day curves, the TDF curves suggest that return levels are increasing for the given return period. While not as distinct with the chosen durations and return periods, as duration increases the trends tend to become linear. While it was found that return levels are significantly increasing, with the inclusion of confidence interval's of 95% it should be considered that significance of these predicted changes were not calculated. Additionally, these curves could have also suffered from overfitting. With those trending upwards, its uncertain if they will continue on this trend. With those trending downwards, there is even more doubt. A similar study could likely benefit from factoring in various location in order to find a distinction between irregularities in a single location and general climate trends. Additionally, since this TDF curve also used the block maxima approach, it similarly could have suffered from a lack of data.

Conclusions

While the results of the nation-wide portion of this study are not robust enough to utilize on their own, they provide a learning experience with which new methodology can be added. The limitations of the nation-wide study were rather unavoidable due to the methodology used. By using the NCDC Climate Divisions dataset, I limited myself to monthly data generalizing conditions for a rather large region. A more thorough study might not only employ additional datasets, but contrast the results. Other studies have shown that models utilizing data from individual stations tend to predict return values significantly more than models using gridded or otherwise interpolated datasets,⁹ however this contrasts with my findings in this study. Additionally, a method could be used to consider the results from individual stations in close proximity to come to a more exhaustive conclusion.

By using the annual block maxima approach, a large amount of data was lost, and with it potentially important information regarding recent extremes.^{5,9} While in a non-stationary conditions additional data will only solidify ones conclusions, in a naturally variable climate additionally impacted by anthropogenic warming, various factors could nullify the trends associated with a specific factor.¹¹

One idea for the future would include fitting data to the Generalized Pareto distribution (GPD) using the peaks-over-threshold (POT) approach. In the same manner the GEV distribution asymptotically approximates the distribution of maxima over a long period, the GPD allows one to approximate the distribution of exceedances over a threshold. This POT process is much more appropriate for studying extremes for a small dataset.^{3,5,6,9} The downside to this approach is asymptotic extreme value theory only holds for weakly dependent data, however, temperature data above a threshold tends to have clusters of highly dependent data. A declustering strategy must be applied to study to negate this issue. One method for this is to use a *peak*-over-threshold approach, which only considers the highest value in a given "peak".⁹

Another option would be to use the point process approach. Similar to the POT approach, this method allows one to express the model in terms of parameters in the GEV distribution. A concern using the POT approach is choosing the ideal threshold. If the threshold is too high, the low level of data will lead to an unreliable result. On the other hand, if the threshold is too low, the tail of the data will not satisfy the convergence criterion. With the point process approach, threshold choice does not directly influence the parameter estimation, rather an ideal threshold should be when parameter estimation stabilizes.^{5,9}

While there is still much room for improvement, this project allowed me explore the potential methods I could utilize in further studies. Using a combination of some of the suggestions above, I hope to continue doing research involving these methods, whether specifically in relation to extreme heat events or other more complex issues involving climate extremes.

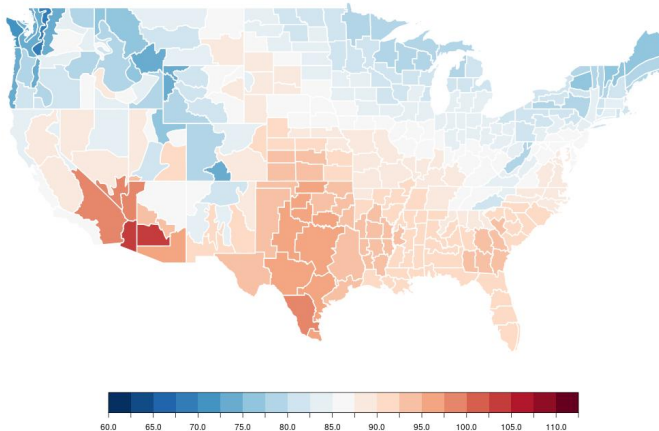
Citations

1. Cheng, L., Aghakouchak, A., Gilleland, E., Katz, R. W. (2014). Non-stationary extreme value analysis in a changing climate. *Climatic Change*, 127(2), 353-369. doi :10.1007/s10584-014-1254-5
2. Cheng, L., Aghakouchak, A. (2014). Nonstationary Precipitation Intensity-Duration-Frequency Curves for Infrastructure Design in a Changing Climate. *Scientific Reports*, 4(1). doi :10.1038/srep07093
3. Coles S (2001). An Introduction to Statistical Modeling of Extreme Values. Springer-Verlag. doi :10.1007/978-1-4471-3675-0.
4. Eckersten, S. (2016). Updating Rainfall Intensity-Duration-Frequency Curves in Sweden Accounting for the Observed Increase in Rainfall Extremes (Master's thesis, Uppsala Universitet). Department of Earth Sciences, Program for Air, Water and Landscape Sciences, Uppsala University, Villavägen 16, SE-751 05 Uppsala. ISSN 1401-5765.
5. Ferreira, A., Haan, L. D. (2015). On the block maxima method in extreme value theory : PWM estimators. *The Annals of Statistics*, 43(1), 276-298. doi :10.1214/14-aos1280
6. Gilleland, E., Katz, R. W. (2016). ExtRemes2.0 : An Extreme Value Analysis Package inR. *Journal of Statistical Software*, 72(8). doi :10.18637/jss.v072.i08
7. IPCC (2012) - Field, C.B., V. Barros, T.F. Stocker, D. Qin, D.J. Dokken, K.L. Ebi, M.D. Mastrandrea, K.J. Mach, G.-K. Plattner, S.K. Allen, M. Tignor, and P.M. Midgley. Managing the Risks of Extreme Events and Disasters to Advance Climate Change Adaptation (pg 8-13, 83, 244-265) .
8. Katz, R. W., Brown, B. G. (1992). Extreme events in a changing climate : Variability is more important than averages. *Climatic Change*, 21(3), 289-302. doi :10.1007/bf00139728
9. Mannshardt-Shamseldin, E. C., Smith, R. L., Sain, S. R., Mearns, L. O., Cooley, D. (2010). Downscaling extremes : A comparison of extreme value distributions in point-source and gridded precipitation data. *The Annals of Applied Statistics*, 4(1), 484-502. doi :10.1214/09-aoas287
10. Meehl, G. A. (2004). More Intense, More Frequent, and Longer Lasting Heat Waves in the 21st Century. *Science*, 305(5686), 994-997. doi :10.1126/science.1098704
11. Myoung, B., Kim, S. H., Kim, J., Kafatos, M. C. (2015). On the Relationship between the North Atlantic Oscillation and Early Warm Season Temperatures in the Southwestern United States. *Journal of Climate*, 28(14), 5683-5698. doi :10.1175/jcli-d-14-00521.1
12. Ouarda, T. B., Charron, C. (2018). Nonstationary Temperature-Duration-Frequency curves. *Scientific Reports*, 8(1). doi :10.1038/s41598-018-33974-y
13. Perkins, S. E., Alexander, L. V., Nairn, J. R. (2012). Increasing frequency, intensity and duration of observed global heatwaves and warm spells. *Geophysical Research Letters*, 39(20). doi :10.1029/2012gl053361
14. Raei, E., Nikoo, M. R., Aghakouchak, A., Mazdiyasni, O., Sadegh, M. (2018). GHWR, a multi-method global heatwave and warm-spell record and toolbox. *Scientific Data*, 5, 180206. doi :10.1038/sdata.2018.206

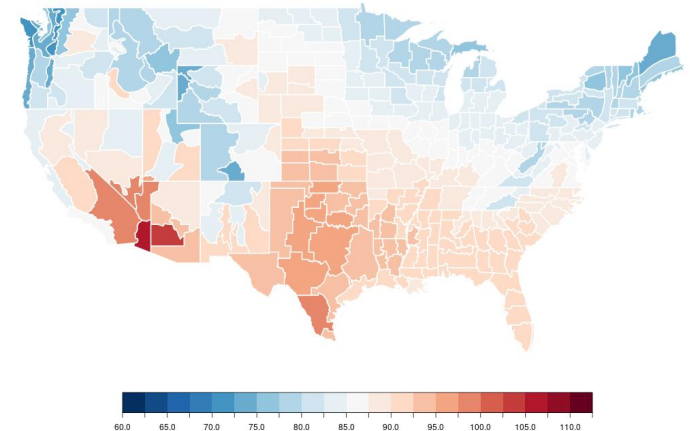
In addition to the prior sources, an innumerable number of other who've shared their programming knowledge through sites such as Stack Overflow and R-bloggers, as well as other individuals who have helped develop the necessary packages to conduct this research.

Appendix

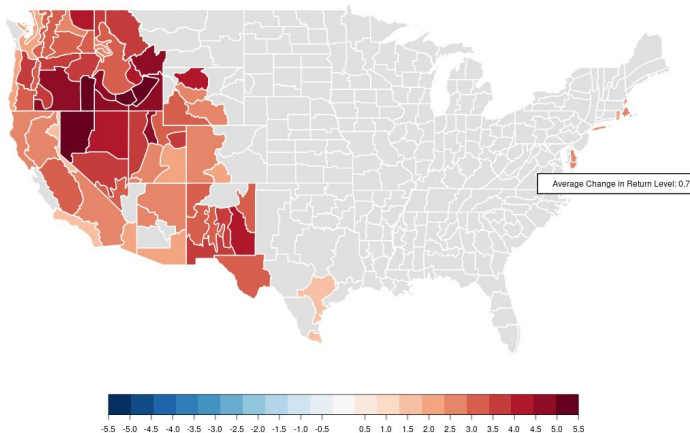
Expected Maximum Return Levels for 2 Years for TMAX in 1978 Using Linear Models



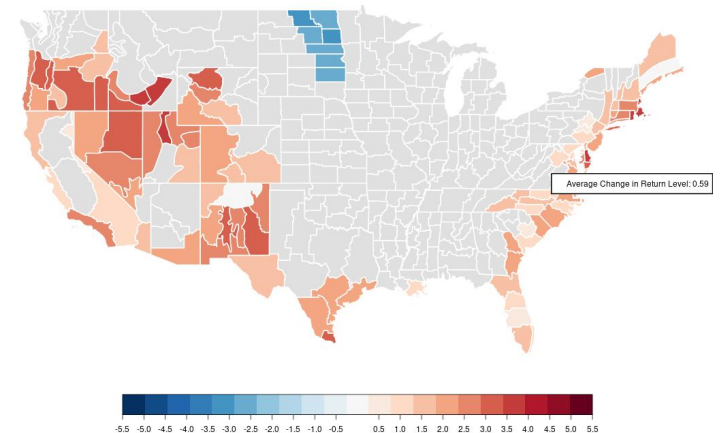
Expected Maximum Return Levels for 2 Years for TMAX in 1958 Using Linear Models



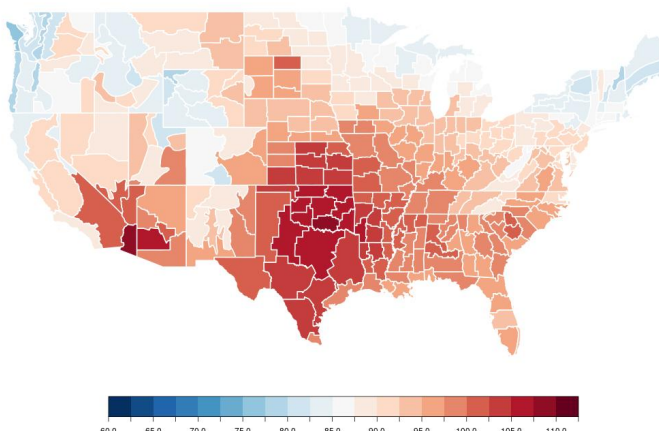
The Change in Expected Maximum TMAX Return Levels for 2 Years Between 1978 and 2018 Using Linear Models



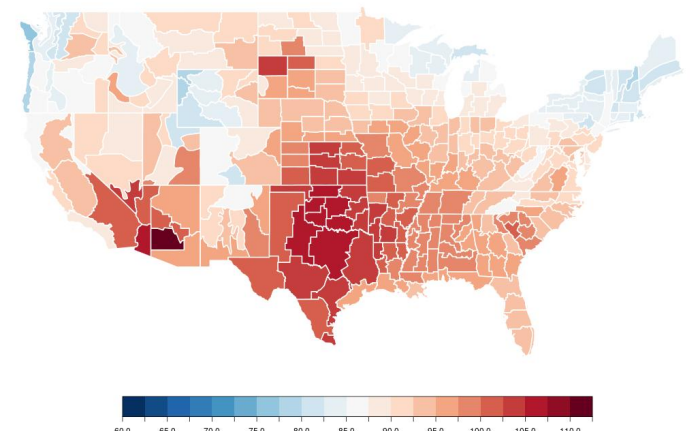
The Change in Expected Maximum TMAX Return Levels for 2 Years Between 1958 and 2018 Using Linear Models



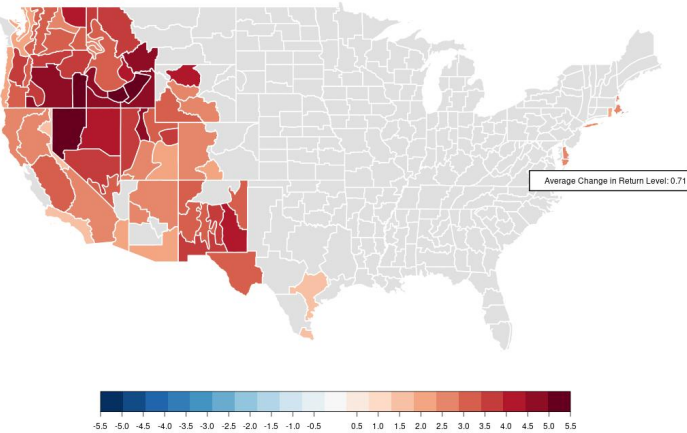
Expected Maximum Return Levels for 100 Years for TMAX in 1978 Using Linear Models



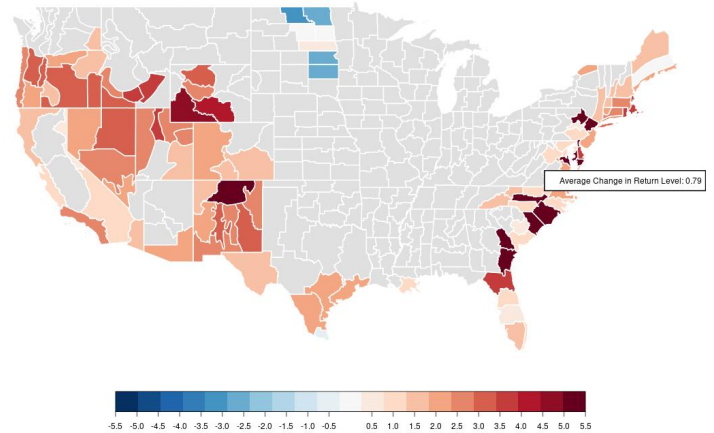
Expected Maximum Return Levels for 100 Years for TMAX in 1958 Using Linear Models



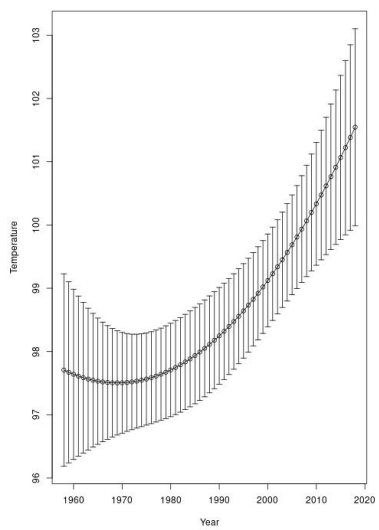
The Change in Expected Maximum TMAX Return Levels for 100 Years Between 1978 and 2018 Using Linear Models



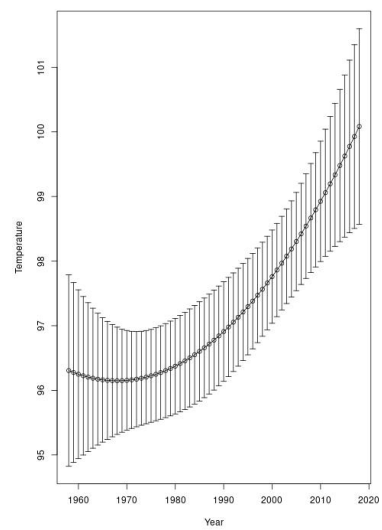
The Change in Expected Maximum TMAX Return Levels for 100 Years Between 1958 and 2018 Using Linear Models



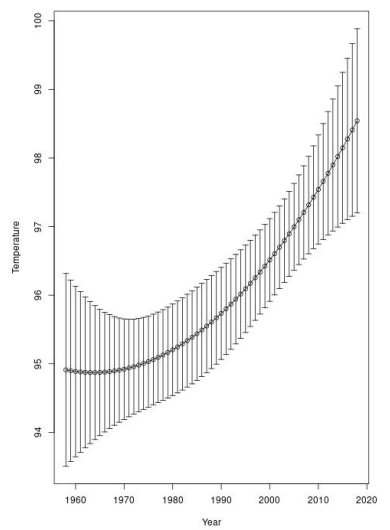
2-Year Return Levels for 1 Day TMAX Events in Houston



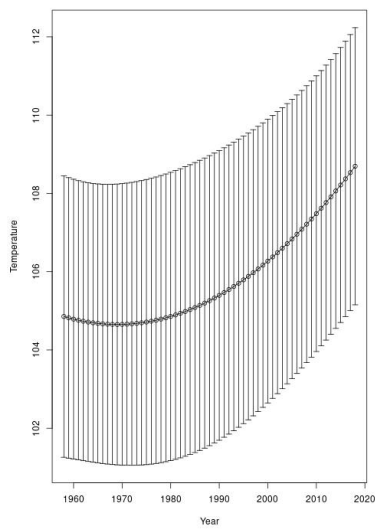
2-Year Return Levels for 3 Day TMAX Events in Houston



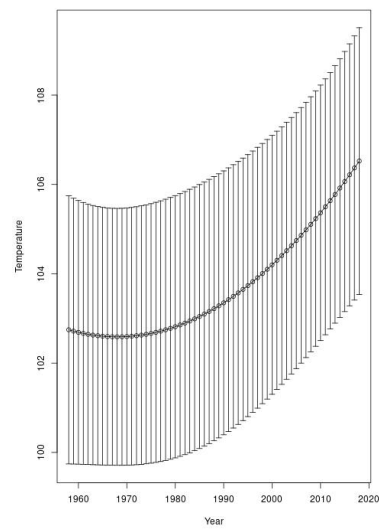
2-Year Return Levels for 7 Day TMAX Events in Houston



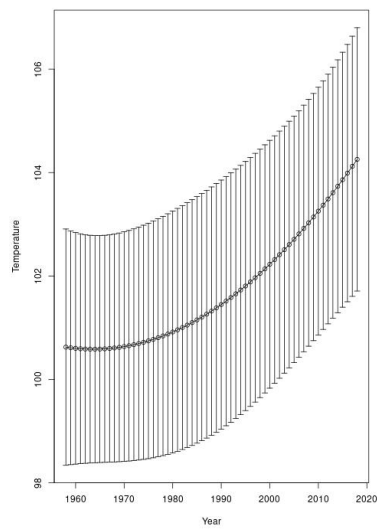
100-Year Return Levels for 1 Day TMAX Events in Houston



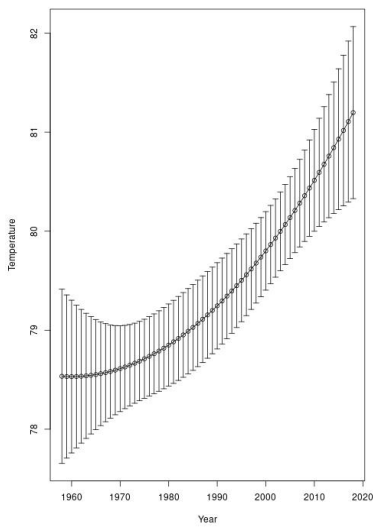
100-Year Return Levels for 3 Day TMAX Events in Houston



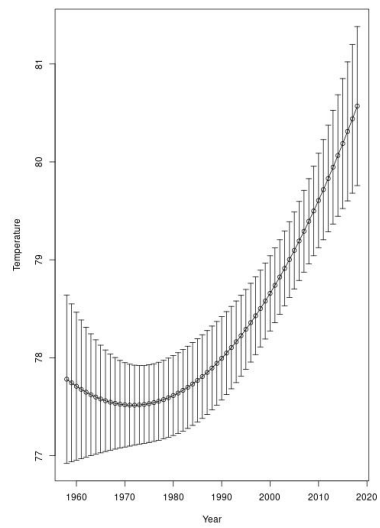
100-Year Return Levels for 7 Day TMAX Events in Houston



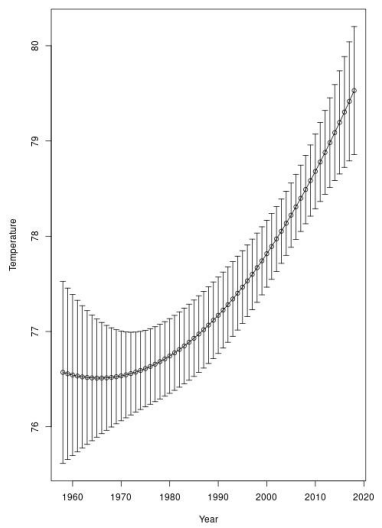
2-Year Return Levels for 1 Day TMIN Events in Houston



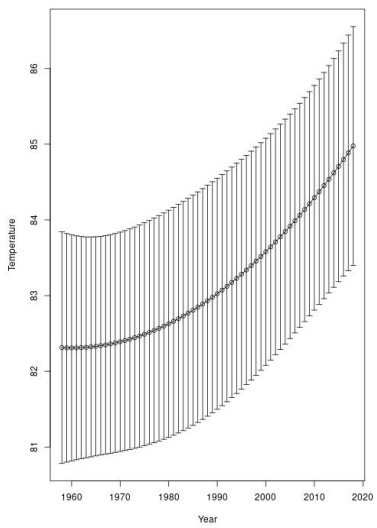
2-Year Return Levels for 3 Day TMIN Events in Houston



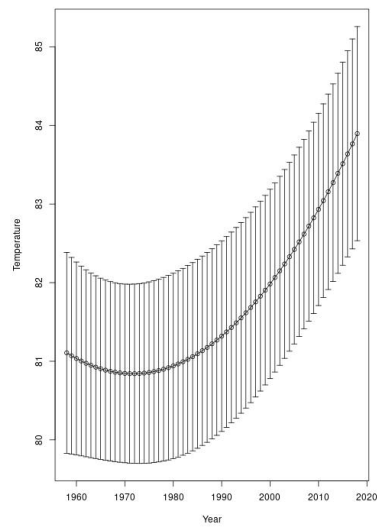
2-Year Return Levels for 7 Day TMIN Events in Houston



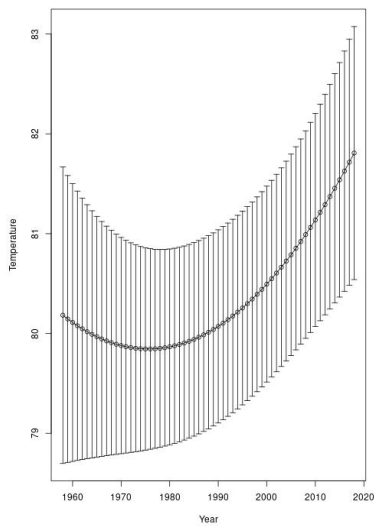
100-Year Return Levels for 1 Day TMIN Events in Houston



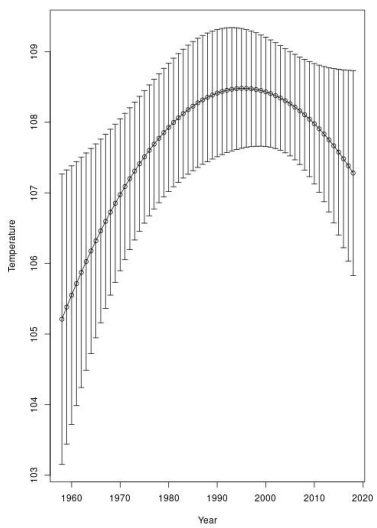
100-Year Return Levels for 3 Day TMIN Events in Houston



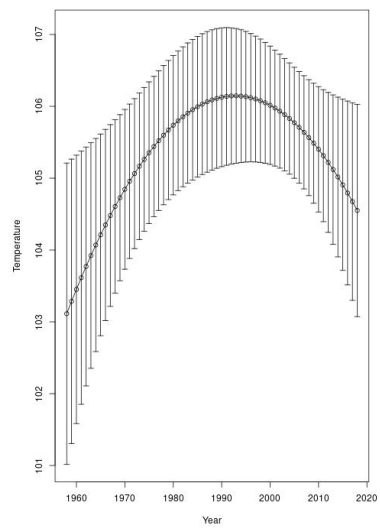
100-Year Return Levels for 7 Day TMIN Events in Houston



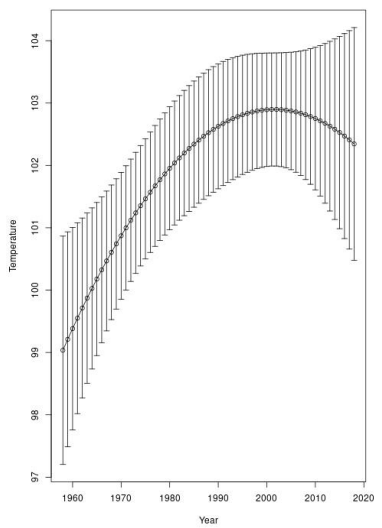
2-Year Return Levels for 1 Day TMAX Events in Sacramento



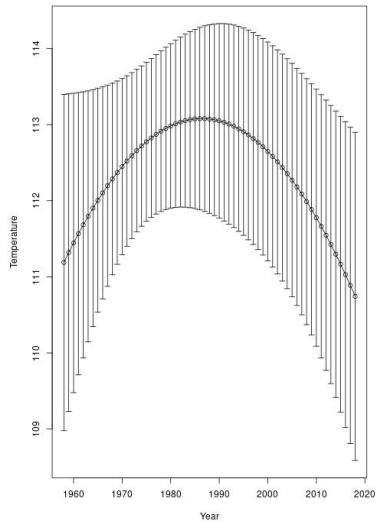
2-Year Return Levels for 3 Day TMAX Events in Sacramento



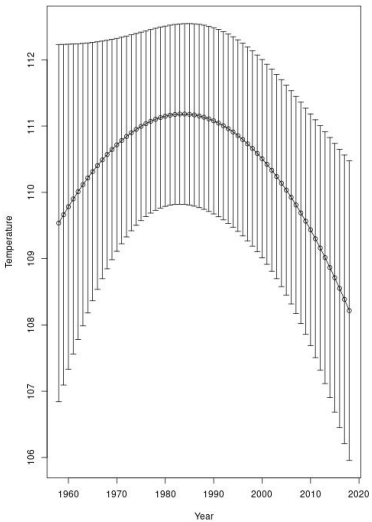
2-Year Return Levels for 7 Day TMAX Events in Sacramento



100-Year Return Levels for 1 Day TMAX Events in Sacramento



100-Year Return Levels for 3 Day TMAX Events in Sacramento



100-Year Return Levels for 7 Day TMAX Events in Sacramento

